Structure of ^{10}Be from the ^{12}C(^{12}C,^{14}O)^{10}Be reaction

H. G. Bohlen,* T. Dorsch, Tz. Kokalova, W. von Oertzen,† Ch. Schulz, and C. Wheldon
Hahn-Meitner-Institut GmbH, Glienicker Str. 100, D-14109 Berlin, Germany
(Received 9 February 2007; published 7 May 2007)

The ^{12}C(^{12}C,^{14}O) two-proton pick-up reaction has been measured at 211.4 MeV incident energy to study the structure of states of ^{10}Be up to excitation energies of 12 MeV. The measured partial angular distributions show pronounced oscillatory shapes, which were described by coupled-reaction-channels calculations. Spin-parity assignments could be derived from these characteristic shapes and two definite assignments have been made. The state at 11.8 MeV has been identified as the 4^+ member of the ground-state band, and the state at 10.55 MeV is assigned $J^\pi = 3^-$. At 5.96 MeV only the 1^-_1 member of the known $2^+_2/1^-_1$ doublet is populated. The angular distribution of the peak at 9.50 MeV, which consists of several unresolved states, has been unfolded using contributions from known states at 9.56 MeV, 2^+, and 9.27 MeV, 4^-. The inclusion of a state at 9.4 MeV reported by Daito *et al.* from the ^{10}B(t,^{3}He)^{10}Be reaction and tentatively assigned (3^+) improved the fit considerably. A K = 2 band is formed with the 2^+_2 state as the band head and the (3^+) state as the second member. The structures of the $K^\pi = 0^+_1$, 2^+_2, and 1^-_1 bands are discussed.

DOI: 10.1103/PhysRevC.75.054604 PACS number(s): 27.20.+n, 21.10.Hw, 21.10.Re, 25.70.Hi

I. INTRODUCTION

In ^{10}Be molecular structures formed by two alpha-particles and two neutrons have attracted much interest. Such cluster structures have been predicted [1–3] and verified in different cluster-model calculations [4–9]. In experimental work a rotational band with the most pronounced molecular structure, based on the particle-stable 0^+ state at 6.179 MeV, has recently been established with three members up to the 4^+ state at 10.15 MeV by Freer *et al.* [10].

However, basic experimental information about the ground-state band in ^{10}Be is still missing: the 4^+ member has not yet been uniquely identified. In an extrapolation from the position of the first 2^+ state at 3.368 MeV the 4^+ member of the ground-state band is expected at an excitation energy of about 11.2 MeV using a $J(J+1)$ dependence of the excitation energies on the spin J. Up to now the observation of a possible candidate is reported by Hamada *et al.* [11], where the state at 11.76 MeV is tentatively assigned (4^+). The excitation energy falls into the expected region, but the fit of the experimental angular distribution with a distorted wave Born approximation (DWBA) calculation is rather poor; a clear spin assignment was not possible. The same state is assigned by Curtis *et al.* [12] as 6^+ (4^+). We conclude that the present experimental situation about the 4^+ member of the ground-state band is rather unsatisfactory.

In theoretical calculations the 4^+ member of the ground-state band is predicted in most of the work cited above for cluster models [4,5,7–9]. In the shell model (SM) the 4^+ state is reported only in no-core shell model (NCSM) calculations [13] and quantum Monte Carlo (QMC) calculations [14]. Calculations within the 1p-shell report only about results up to 3^+ states [15,16].

In this work we selected the ^{12}C(^{12}C,^{14}O)^{10}Be two-proton pick-up reaction for the spectroscopy of ^{10}Be for several reasons:

(i) The ground state of ^{10}Be is strongly deformed ($\beta_2 = 1.13$ [17]). To populate the 4^+ state of the *ground-state band* both, protons and neutrons, have to be excited to 2^+ configurations, which are then coupled to the deformed state with total spin 4^+. In the two-proton pick-up reaction on ^{12}C the corresponding proton 2^+ configuration can be directly created by the pick-up mechanism. This transition must be combined in a two-step mechanism with the inelastic excitation of the ^{12}C target nucleus to the first 2^+ state, which contains the corresponding 2^+ components on the neutron side. The strong inelastic 2^+_1 excitation of ^{12}C takes place as the first step, followed by the two-proton pickup to ^{10}Be(4^+) in a second step.

(ii) In the two-proton transfer from the ^{12}C projectile to final states of ^{14}O only the ground state of ^{14}O is particle stable. Any excited state of ^{14}O populated in this reaction will already decay in flight and will not reach the detector.

(iii) In the *projectile transition* between the ground states of ^{12}C(0^+) and ^{14}O(0^+) only the angular momentum transfer of $\ell = 0$ is allowed, the proton pair is coupled to $S = 0$. In this sense this reaction is comparable to the (n,^{3}He) or (p,t) reactions. The total angular momentum transfer ℓ to final states of ^{10}Be is determined completely by the *target transition* $^{12}\mathrm{C}(0^+) \rightarrow {}^{10}\mathrm{Be}(E_x, \mathrm{J}^\pi)$. The angular distributions will therefore show the characteristic pattern of the ℓ-values for these target transitions. This concerns for example the *phase* of the oscillatory structure and the *position of the first deep minimum* in the diffraction pattern of the angular distribution.

(iv) Finally, with ^{14}O as the outgoing particle we always observe a relatively weak three-body background compared to other two-proton pick-up reactions [18].

*Electronic address: bohlen@hmi.de
†Also Freie Universität Berlin, Fachbereich Physik, Arnimallee 14, D-14195 Berlin, Germany.

We also want to mention that projectile and target are identical bosons (^{12}C). For this reason the transition amplitude of the reaction has to be symmetrized and only even partial waves are in the entrance channel.

With these characteristics, the ^{12}C(^{12}C,^{14}O) reaction is a rather sensitive tool for spin-parity assignments, and we expect to be able to identify the 4^+ member of the ground-state band and also to obtain more information about the structure of other states of ^{10}Be.

The paper is organized as follows. In Sec. II the details of the measurements are given. In Sec. III the results are shown and discussed in detail, i.e., the mechanism for the population of final states in the two-proton pickup. Section III B is dedicated to the discussion of odd-parity states and unnatural-parity states ($\pi = (-1)^{J+1}$). Coupled-channels calculations have been performed for a quantitative description of the data, they are presented in Secs. III C and III D. The band structures of ^{10}Be are discussed in Sec. III E, and the conclusions follow in Sec. IV.

II. MEASUREMENTS

The measurement of the ^{12}C(^{12}C,^{14}O)^{10}Be reaction has been performed at the Q3D magnetic spectrograph of the ISL ion-beam laboratory at the Hahn-Meitner-Institut, Berlin. The cyclotron delivered the ^{12}C beam with the energy of 211.4 MeV. A ^{12}C target of 200 μg/cm^2 thickness has been used. Reaction products were identified in the focal plane of the spectrograph in a detector system, which consists of a gas-filled chamber, where the energy-loss (ΔE) and the position ($X1$) of the particles are measured, and a scintillator bar behind it for the rest energy (E) and a fast timing signal to trigger the start of the time-of-flight (ToF) measurement [18]. The stop signal could be taken from the cyclotron RF, since the width of the beam bunches was only 0.7 ns, which made an extra fast-timing detector unnecessary. With this method a total resolution of 1 ns was achieved for the time-of-flight. Isotopes were uniquely separated in plots of ΔE versus E and ToF, respectively.

The position $X1$ has been measured using the delay-line read-out technique. A structure of 470 strips with 2 mm pitch along the focal plane is connected to a tapped delay-line with 5 ns delay between the taps. The measured delay time of the signals to both ends of the delay-line is used to calculate the position $X1$. This method also interpolates the position between the taps, because the primary signal of an event is extended over about four strips, and the center-of-gravity of the distribution is taken. Typically a relative momentum resolution of 4×10^{-4} is achieved.

In the actual measurement, however, the large energy-loss difference between incoming ^{12}C and outgoing ^{14}O particles in the ^{12}C target contributes to the line width by additional 250 keV, resulting in a total width for the resolution of 350 keV FWHM for the ^{14}O exit channel. The excellent time resolution allowed us to deduce from the correlation between scattering angle, θ_L (within the range of 4° of the aperture opening) and the time-of-flight along the trajectories to the focal plane a transformation from ToF to θ_L with an angular resolution of about 0.3°. Details of the ion-optical imaging of the Q3D-spectrograph are given in [19].

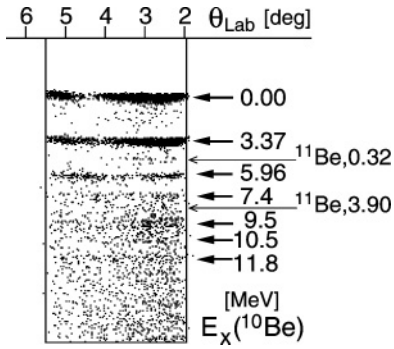

FIG. 1. Two-dimensional plot of events from the ^{12}C(^{12}C, ^{14}O)^{10}Be reaction at an incident energy of 211.4 MeV in a diagram of the scattering angle θ_{lab} on the horizontal axis and the position in the focal plane of the Q3D magnetic spectrograph on the vertical axis. The excitation energies of observed states of ^{10}Be are indicated.

The good angular resolution is illustrated in Fig. 1 in a two-dimensional plot of focal-plane position $X1$ versus ToF gated by outgoing ^{14}O particles. The states of the recoil nucleus ^{10}Be are clearly seen, and the angular modulation of the cross sections as well. With the projection on the position axis the excitation energy spectrum shown in Fig. 2 is obtained. A second angular range has been measured from 3.5° to 7.5° with the Q3D spectrograph at an angular setting of $\theta_{lab} = 5.5°$.

In Fig. 2 one can see that the ground state and first excited 2^+_1 state are populated the strongest (a characteristic feature for pick-up reactions at these incident energies). As we will show in the analysis, most of the other states observed up to 11.8 MeV excitation energy are populated in two-step processes, which immediately leads to lower cross sections for the transitions. Two contamination lines from the natural ^{13}C content of carbon material (1.1%) are observed in the spectrum, populating states of ^{11}Be at excitation energies of 0.32 MeV and 3.90 MeV (indicated in Figs. 1 and 2). From

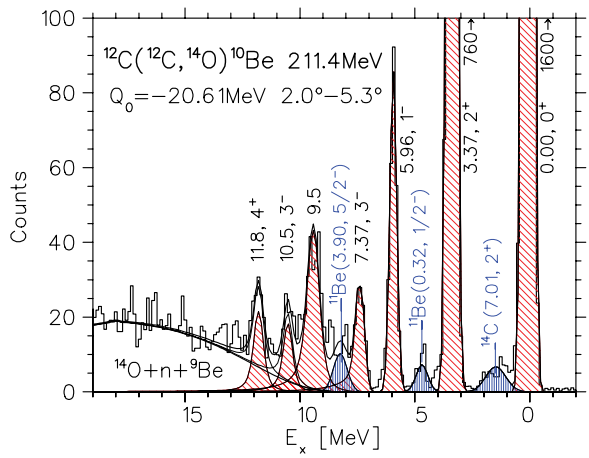

FIG. 2. (Color online) Spectrum of the two-proton pick-up reaction ^{12}C(^{12}C,^{14}O)^{10}Be at $E_{lab} = 211.4$ MeV and $\theta_{lab} = 3.5°$. States of ^{10}Be are marked by downward hatched areas, and contamination lines are indicated explicitly.

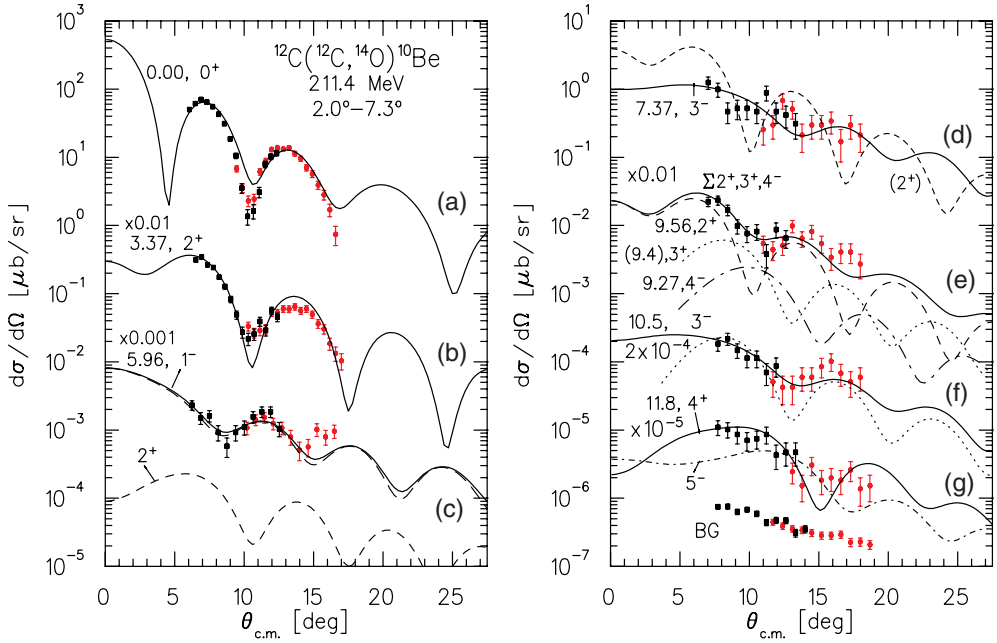

FIG. 3. (Color online) Angular distributions of the ^{12}C(^{12}C,^{14}O) reaction to the ground state (a) and excited states, (b)–(g), of ^{10}Be. Excitation energies are given in MeV on the left together with spins and parities and the scale factors for the plot on a common scale. The lines correspond to results from coupled-channel calculations using the code FRESCO [25]. Long-dashed, short-dashed, long-dot-dashed, and short-dot-dashed lines in (c), (d), (e), (g) show angular distributions for 1^-, 2^+, 4^-, and 5^- states, respectively. In (e) a fit with contributions from 2^+, 3^+, and 4^- states is shown (see text), and in (f) also the shape for a 3^+ angular distribution (dotted line) for comparison. BG represents the shape of the background angular distribution.

a small oxygen contamination in the target a kinematically broadened line from the excited 2_1^+ state of ^{14}C at 7.01 MeV is also visible in the spectrum, just between the ground state and 2_1^+ lines of ^{10}Be. A continuous three-body distribution with the three particles ^{14}O (detected), ^{9}Be and one neutron (not-detected) in the exit channel rises at about 9 MeV see Fig. 2). This background results from two possible mechanisms, (i) the neutron knockout from the projectile followed by the two-proton pickup and (ii) a sequential in-flight decay process. The corresponding processes are discussed in Ref. [18].

In the fit of the spectrum Gaussian line shapes with a resolution of 350 keV FWHM are used for the particle-stable states of ^{10}Be, and for the states above the neutron threshold ($S_n = 6.81$ MeV), Breit-Wigner line shapes are folded with the resolution (if known, the corresponding decay widths are taken from Ref. [20]). The positions of the seven observed peaks attributed to states of ^{10}Be have been fitted with these profiles to identify the excitation energies as given in Fig. 2. The values correspond to known states [20] of ^{10}Be within the resolution. The peaks at 5.96 MeV, 7.37 MeV, and 9.5 MeV may contain several unresolved states due to the broad experimental line widths. In these cases the calculated characteristic shapes of angular distributions of the unresolved states are used to disentangle the contribution of each state to the measured sum (see the following section).

The angular distributions were projected for each peak from the two-dimensional calibrated plots of excitation energy versus scattering angle (Fig. 1) with a gate around the region of the visible line. In the excitation energy region of 16 MeV the background has also been projected with a width of 3 MeV for comparison, to show the shape of the background angular distribution. Almost all of the observed states were not disturbed by the three-body background (Fig. 2). For the 11.8 MeV state a background of 40% with the angular shape of the experimental background has been subtracted from the projected angular distribution. The angular calibration has been performed using the angle of the center of the aperture opening, defined by the angle of the Q3D spectrograph, and both edges of the aperture giving the scale factor for the transformation.

The corresponding experimental angular distributions are shown in Figs. 3(a)–3(g), (BG). The data shown as squares correspond to the angular setting of the magnetic spectrograph at 3.5°, and the circles to the setting at 5.5°. The error bars represent statistical errors only.

III. RESULTS AND DISCUSSION

The results obtained from the analyis of the angular distributions shown in Fig. 3 are given in Table I together with results from a selected number of other reactions, which are relevant for comparison: (i) the one-proton pick-up reaction ^{11}B(d,^{3}He) [21], (ii) the ^{7}Li(α, p) reaction [11] and (iii) the charge-exchange reaction ^{10}B(t,^{3}He) [22] (for the ^{10}B(d,^{2}He) reaction see Ref. [23]). Before the details are described we want to make some remarks about the *observed shapes* of the angular distributions.

A. Shape of experimental angular distributions

The angular distributions from the first three peaks of the ^{10}Be spectrum (Fig. 2) show very pronounced oscillatory

TABLE I. Comparison of results obtained in this work with those of the one-proton pickup ^{11}B(d,^{3}He), the ^{7}Li(^{4}He,p) reaction, the charge-exchange reaction ^{10}B(t,^{3}He) and the compilation of Tilley *et al.* for ^{10}Be. Results of the coupled-channels calculations are given in columns 4 to 7. The quantities δ_ℓ and A_ℓ are the deformation lengths (Sec. III C) and spectroscopic products (Sec. III D), respectively. Underlined A_ℓ-values are adjusted in the fit to the data, an error of 5–8% is estimated.

	^{12}C(^{12}C,^{14}O$_{g.s.}$)^{10}Be(E_x, J^π)						^{11}B(d,^{3}He)			^{7}Li(α, p)		^{10}B(t,^{3}He)		Tilley *et al.* (2004)	
	E_L=211.4 MeV (present work)						52 MeV [21]			68 MeV [11]		381 MeV, 0° [22]		[20]	
No	E_x, Γ [MeV]	J^π	steps in the CRC-calc. (Fig. 4)				E_x [MeV]	J^π	S	E_x [MeV]	J^π	J^π	B(GT)	E_x [MeV]	J^π
			step 1		step 2										
			$\ell/E\lambda$	A_ℓ/δ_λ	$\ell/E\lambda$	A_ℓ/δ_λ									
1	0.00	0^+_1	$\ell=0$	1.20			0.00	0^+	0.65	0.00	0^+			0.000	0^+
2a	3.37(5)	2^+_1	$\ell=2$	1.00			3.37	2^+	2.03	3.37(5)	2^+	2^+	0.08(3)	3.368	2^+
2b			$\ell=0$	1.20	$E2$	2.0[d]									
3a	5.96(5)	2^+_2	$\ell=2$	⩽0.25			5.96	2^+	0.13	5.98(5)	2^+	2^+	0.95(13)	5.958	2^+
3b			$E2$	−1.80[d]	$\ell=0,2$	0.25									
4a	5.96(5)	1^-	$E3$	0.90[d]	$\ell=2$	1.00								5.960	1^-
4b			$\ell=1$	−0.30											
5a	7.37(5), 0.05(5)	3^-_1	$E3$	0.90[d]	$\ell=0,2$	0.63				7.37(5)	3^-			7.37	3^-
5b			$\ell=3$	−0.30											
	7.54	2^+_3	not obs.	<0.3											
	Peak at 9.5 MeV:														
6	9.27(10)[a]	(4^-)	$E3$	0.90[d]	$\ell=2$	1.06				9.27(5)	(4^-)			9.27	(4^-)
7	(9.4(10))[a]	(3^+)	$E2$	−1.80[d]	$\ell=2$	(0.92)						$(2^+,3^+)$	0.31(8)		
8	9.56(8)[a]	2^+_4	$\ell=2$	1.11			9.60	2^+	1.19	9.64(7)	(2^+)			9.56	2^+
9a	10.55(10), 0.2(1)	3^-_2[b]	$E3$	0.90[d]	$\ell=0,2$	0.80				10.57(7)	⩾1			10.57	⩾1
9b			$\ell=3$	−0.30											
10		(3^+)[c]	$E2$	−1.80[d]	$\ell=2$	(1.54)									
11	11.8(1), 0.2(1)	4^+[b]	$E2$	−1.80[d]	$\ell=2$	1.90				11.76(7)	(4^+)			11.76	(4^+)

[a]Decomposition into the three $2^+/3^+/4^-$ components, see section III D3 and Fig. 3.
[b]This work.
[c]A tentative (3^+) assignment cannot be completely excluded (see text).
[d]References [17,20,33–36].

structures (Fig. 3, left panel) in agreement with the expectations discussed in the introduction. While the oscillations of the ground state (0^+) and first excited state (2^+_1) are in phase and signify *even* parity, the oscillatory structure of the angular distribution at 5.96 MeV [Fig. 3(c)] is out-of-phase with the others. It is well known [24] that at this excitation energy a $2^+_2/1^-$ doublet exists with a separation energy between the states of only 1.5 keV [20]. The out-of-phase behavior with the distributions of the 0^+ and 2^+ states indicates, that the 1^- state of the doublet is observed here. The cross sections for the second 2^+ state are obviously very small, as this will be shown later more quantitatively by the decomposition of the measured angular distribution.

The next populated state observed in the spectrum at 7.37 MeV is well known as a 3^- state. An oscillatory structure of the angular distribution is hardly seen due to low statistics. If the neighboring 2^+_3 state at 7.54 MeV (170 keV separation) would contribute significantly to the peak, its center-of-gravity should be shifted more to higher excitation energies, but this is not the case. For this reason we conclude, that the 7.54 MeV state must be much weaker as compared to the 3^- state at 7.37 MeV.

For the peak at 9.5 MeV, two or three states may contribute to the experimental angular distribution: a 4^- state at 9.27 MeV [20], furthermore a tentative state at 9.4 MeV [22], which is considered as a good candidate for a 3^+ state [16], and a well established 2^+ state at 9.56 MeV [20]. The oscillatory structure of the experimental angular distribution is in phase with the one for the ground and first excited states of ^{10}Be. Therefore the dominant component must be the 2^+ state at 9.56 MeV. The 3^+ state, although of even parity, would show an out-of-phase behavior with respect to the 2^+ state due to its unnatural parity, as will be seen also from the coupled-channels calculations.

B. Direct transitions, odd-parity states, and two-step mechanism

The observed states are populated either (i) in a one-step direct transfer of the proton pair, (ii) by a two-step reaction mechanism or (iii) by both mechanisms in different transfer branches. In all cases the protons of the pair are coupled to $S = 0$ with antiparallel spin orientation. This coupling is conditioned by the transition from the ^{12}C projectile to the ^{14}O outgoing particle, because otherwise the 0^+ ground state of ^{14}O is not formed. In this reaction the ^{14}O ground state is described as an $S = 0$ proton-pair bound in an $\ell = 0$ orbit to the ground state of ^{12}C as the core. The $S = 0$ coupling

of the transferred proton-pair also restricts the possible hole configurations created in the ^{12}C target nucleus. In the direct pickup from the 1p-shell only hole states with $J = 0^+$ and 2^+ can be created in ^{10}Be, and only $\ell = 0$ or $\ell = 2$ angular momentum transfers are possible in the direct one-step process. The transitions to the ^{10}Be ground state, to the first excited 2^+ state at 3.37 MeV and to the 2^+_4 state at 9.56 MeV can be described in this way. The 0^+_2 and 2^+_3 states at 6.18 MeV and 7.54 MeV, respectively, which are members of the molecular band of ^{10}Be [10], are not observed and therefore not considered in the following discussion. The 2^+_2 state at $E_x = 5.96$ MeV could be populated in a direct one-step process, but the cross section observed for the unresolved $2^+_2/1^-_1$ doublet is dominated by that of the 1^-_1 state.

The odd-parity 1^- state at 5.96 MeV and also the observed 3^- states may be populated in a direct proton-pair transfer, when ground state correlations in the ^{12}C target with $(2s1d)^2$ admixtures (2p-2h excitations) are taken into account. The pick-up of one proton from the (2s1d)-shell and the other one from the (1p)-shell could populate in this case odd-parity states in ^{10}Be with ℓ-values of $\ell = 1$ or $\ell = 3$ for the transfer of the proton-pair. But (sd)-shell admixtures in the ground state of ^{12}C are weak [26–29]. Simmonds *et al.* [26] found in the ^{12}C$(t, \alpha)^{11}$B reaction for the proton pickup from ^{12}C to $5/2^+$ and $1/2^+$ final states of ^{11}B maximal spectroscopic factors of $C^2S = 0.14 \pm 0.07$. This value is used later in the coupled-channels calculations to estimate the maximum contributions from the *direct* two-proton pickup in the population of odd-parity states of ^{10}Be. There must exist other, stronger contributions from the two-step mechanism via the inelastic excitation of the 3^- state of ^{12}C at 9.64 MeV in the first step and the two-proton pick-up with $\ell = 2$ or $\ell = 0$ and 2 angular momentum transfers to the final state of ^{10}Be in the second step.

The 1^- state at 5.96 MeV is known as the band head of an odd-parity band with further members 2^- ($E_x = 6.26$ MeV), 3^- (7.37 MeV) and 4^- (9.27 MeV). The structure of this band is known from the one-neutron transfer on ^{9}Be [30,31], where all the four band members are very strongly populated with a large single-particle strength. The structure corresponds to an intrinsic configuration of one neutron in a 2s1/2 or 1d5/2 orbit coupled to the ^{9}Be$_{g.s.}(3/2^-)$ core, a $1\hbar\omega$ (1p-1h) excitation with respect to the ground state of ^{10}Be.

The excitation of states with unnatural parity like 4^- or 3^+ definitely requires a two-step mechanism. These states can be reached via an inelastic excitation of ^{12}C to the first 3^- or 2^+ states, respectively, followed by the two-proton pick-up with an angular-momentum transfer $\ell = 2$. These two-step transitions are supported by the very large inelastic cross sections for the corresponding states of ^{12}C.

Finally it is expected that the population of the 4^+ state of the ground-state band, which results from excitations of the neutrons as well as the protons to 2^+ configurations in the 1p-shell, is also only reached via a two-step process.

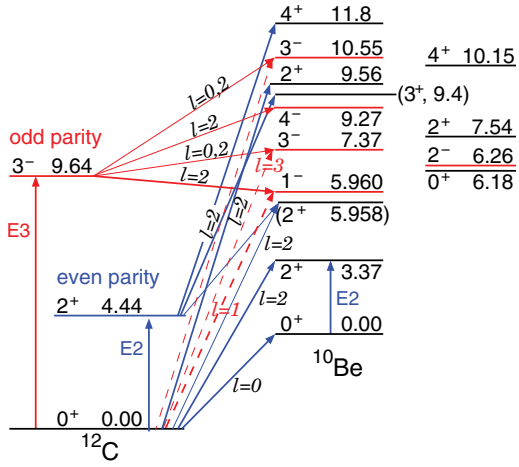

FIG. 4. (Color online) Coupling scheme used in the coupled-reaction-channels calculations for the two-proton transfer from ^{12}C to final states of ^{10}Be for even and odd parities (schematic). Known states of ^{10}Be below 12 MeV, which have not been observed in this reaction, are plotted on the right.

C. Coupled-reaction-channels calculations

From the discussion above it is clear, that the reaction mechanism and the experimental angular distributions can only be described by coupled-reaction-channels calculations (CRC), where the different steps in the reaction are explicitly taken into account. In principle the transfer of the two protons can be treated in two different ways: (i) either as a sequential pick-up of the two protons via intermediate states of ^{11}B to final states of ^{10}Be with all possible couplings, or (ii) as the transfer of a proton pair, coupled to $S = 0$, from the ^{12}C target to the 0^+ ground state of the outgoing particle ^{14}O. For the latter case the population of the observed states of ^{10}Be has been already discussed in the preceding section.

In the first case the many intermediate states in ^{11}B will lead to a large number of couplings and transition branches, which makes a reliable quantitative description very difficult. In the second case, besides the direct proton-pair transfer, only the inelastic transitions in ^{12}C to the 2^+ state at 4.44 MeV and to the 3^- state at 9.64 MeV, and in ^{10}Be to the 2^+_1 state, have to be taken into account as intermediate states, and the strengths of the corresponding excitations are known.

We have chosen the latter method to perform the CRC calculations using the code FRESCO [25]. The relevant transitions with all the branches from the ^{12}C ground state to the final states of ^{10}Be are shown in Fig. 4, details will be discussed in the next section.

The calculations have been performed with an optical potential obtained by Fulmer *et al.* [32] (potential WS2) from the analysis of elastic and inelastic scattering data for the scattering system ^{9}Be+^{12}C at almost the same incident energy-per-nucleon as for the present case (17.6 MeV/nucleon). Woods-Saxon (WS) form factors are used for the real and imaginary parts of the optical potential with the following parameters: Real part: $V_0 = 243.4$ MeV, $r_0 = 0.564$ fm, $a_r = 0.932$ fm. Imaginary part: $W_i = 33.3$ MeV, $r_i = 0.982$ fm, $a_i = 0.960$ fm. Coulomb potential: $r_C = 1.20$ fm.

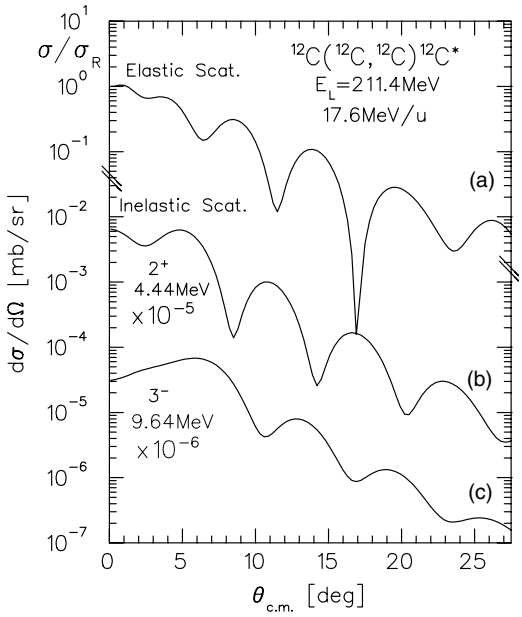

FIG. 5. Calculated angular distributions of the elastic (a), and inelastic scattering (b), (c), of ^{12}C on ^{12}C at 211.4 MeV incident energy.

The different radii of the potentials are defined as $R_x = r_x(A_1^{1/3} + A_2^{1/3})$, where $r_x (x = 0, i, C)$ is the radius parameter of the corresponding part of the potential and A_1 and A_2 the masses of the projectile and target, respectively.

The calculated angular distributions of the elastic scattering and the inelastic excitations to the 2_1^+ state at 4.44 MeV and to the 3_1^- state at 9.64 MeV are displayed in Fig. 5. The latter angular distributions have been calculated in the collective model using deformation lengths $\delta_\lambda = \beta_\lambda R$ with the multipolarities λ, the deformation parameters β_λ and the radius R$= 1.2 \times A^{1/3}$ fm of the nucleus (A is the mass number).

The values of the deformation lengths δ_λ have been taken from the literature. These are for the $E2$ and $E3$ transitions in ^{12}C [17,20,33,34]: ^{12}C$(0_1^+ \rightarrow 2_1^+)$, $\delta_2 = -1.80$ fm (the minus sign results from the oblate deformation of the state), ^{12}C$(0_1^+ \rightarrow 3_1^-)$, $\delta_3 = 0.90$ fm.

For the ^{10}Be$(0_1^+ \rightarrow 2_1^+)E2$ excitation the value $\delta_2 = 2.00$ fm has been used in accordance within the error bars with the δ_2 values obtained in the range from 1.84 fm to 1.99 fm from inelastic proton scattering on ^{10}Be [35], and in a more recent experiment, from ^{10}Be scattering on protons, $\delta_2 = 1.80(25)$ fm [36]. These values are systematically lower than the ones derived from life-time measurements [$\tau = 181(21)$ ps] [17], which yield a mean value of $\delta_2 = 2.9(2)$ fm using $R = 1.2 \times (10)^{1/3}$ fm.

D. Transitions and transfer branches

1. *Transitions to the 0$^+$ ground state and the 2$^+$ states*

The experimental angular distributions are compared with the results of the coupled-channels calculations in Fig. 3. To reproduce the experimental cross sections the spectroscopic amplitudes for the transitions to all final states given in Table I have been adjusted to obtain an optimum fit to the experimental data simultaneously. The channel coupling made several iterations necessary. The varied quantities A_ℓ (Table I) represent the *product of spectroscopic amplitudes for the proton-pair in the initial and the final state* (the latter is in all cases the ground state of ^{14}O). In the following we will use the term *spectroscopic product* for A_ℓ to express that this is a product of two spectroscopic amplitudes.

The A_ℓ-values are given in columns 5 and 7 of Table I together with the angular momentum transfers ℓ (columns 4 and 6) for the corresponding steps of the transfer reaction. As discussed in the first part of Sec. III B the states with spin 0^+ and 2^+ can be populated in ^{10}Be in a *direct* one-step process. The corresponding A_ℓ-values have been determined for the transitions to the following states: 0^+, 0.00 MeV; 2_1^+, 3.37 MeV; 2_4^+, 9.56 MeV (see Table I, rows 1, 2a, and 8, respectively). For the 2_2^+ state at 5.96 MeV only an upper limit of $A_{\ell=2} \leqslant 0.25$ could be estimated (row 3a). The 0_2^+ state at 6.18 MeV and 2_3^+ state at 7.54 MeV, which are members of the molecular rotational band [10], were not observed.

The *fitted* A_ℓ-values are underlined in Table I to indicate, that they were used as free parameters in the fit to the data. All not-underlined values, as for example in row 2b, have been kept constant. They were determined already before in another transition or, as in all cases of the deformation lengths δ_ℓ, were taken from the literature [17,20,33–36]. Figure 4 shows the coupling scheme used in the calculations.

The fits to the angular distributions of the ^{10}Be ground state and the first excited 2^+ state at 3.37 MeV are shown in Fig. 3(a) and (b), respectively. In the population of the 2_1^+ state the two branches, namely (i) the one-step direct transfer of the proton pair to this state (row 2a in Table I) and (ii) the transition via the ^{10}Be ground state followed by the $E2$ excitation in ^{10}Be (row 2b), are very strong. An additional feeding via the $E2$ excitation of the first excited 2^+ state of ^{12}C is much weaker and has not been included in the final calculation.

The experimental spectroscopic products for the transitions to the ground state, $A_{\ell=0} = 1.20(6)$, and to the first excited state, $A_{\ell=2} = 1.00(5)$, can be compared to results from SM calculations. Cohen and Kurath [37] have tabulated spectroscopic factors SMAG and DMAG (this terminology is used by the authors of Ref. [37]) for two-nucleon transfers with $S = 0$ on 1p-shell nuclei for the angular momenta $\ell = 0$ (SMAG) and $\ell = 2$ (DMAG), respectively. The ground state transitions for the projectile from ^{12}C(0^+) to ^{14}O(0^+) and for the target from ^{12}C(0^+) to ^{10}Be(0^+) have the values SMAG(proj) $= 0.60$ and SMAG(targ) $= 2.75$, respectively. From this a spectroscopic product of $A_{\ell=0}^{SM} = \sqrt{0.60 * 2.75} = 1.28$ is calculated, which is in excellent agreement with the experimental value of 1.20(6) (Table II).

The SM spectroscopic factor for the transition to the 2_1^+ state is DMAG$= 1.22$ [37]. Also in this case the theoretical value of $A_{\ell=2}^{SM} = \sqrt{0.60 * 1.22} = 0.86$ is very close to the experimental value $A_{\ell=2} = 1.00(5)$ obtained in this analysis.

This good agreement for the spectroscopic product of the 2_1^+ state is achieved in an even more complicated situation, where a second independent transition branch with no adjustable parameters (see row 2b in Table I) contributes coherently to the final cross section. This second branch corresponds to

TABLE II. Comparison of excitation energies E_x, spectroscopic amplitudes $\sqrt{S}$ from the ^{11}B(d,^{3}He)^{10}Be reaction and spectroscopic products A_ℓ of the ^{12}C(^{12}C,^{14}O$_{g.s.}$)^{10}Be reaction with results from SM calculations within the 1p-shell [37].

Reference [20]		[21] this work		SM calcul. [37]	
J^π	E_x [MeV]	$\sqrt{S}$ exp.	A_ℓ exp.	A_ℓ^{SM} calc.	E_x^{SM} [MeV]
0_1^+	0.000	0.81	1.20(6)	1.28	0.00
2_1^+	3.368	1.42	1.00(5)	0.86	4.16
2_2^+	5.958	0.36	$\leqslant$0.25	0.05	9.16
2_4^+	9.56	1.09	1.11(8)	1.65	5.81

a two-step transition via the ground state of ^{10}Be (Fig. 4), where the spectroscopic product in the first step is already fixed by the fit to the ground state angular distribution. For the second step the strength of the inelastic excitation to the 2_1^+ state of ^{10}Be is fixed by the deformation length $\delta_2 = 2.0$ fm taken from the literature [20,35]. We can say that the cross sections for the ground state and first excited state of ^{10}Be are reproduced quantitatively by the shell-model spectroscopic factors of Cohen and Kurath [37].

In Table II also experimental spectroscopic amplitudes $\sqrt{S}$ (S spectroscopic factor) for the one-proton pickup from ^{11}B [21] are given for comparison. The values show a similar trend as the spectroscopic products A_ℓ from the present measurement, especially for the 2^+ states at 5.96 MeV and 9.56 MeV (also in Ref. [21] the 2_3^+ state at 7.54 MeV was not observed). But the SM calculations [37] completely fail to reproduce the experimental spectroscopic products for the 2_2^+ and 2_4^+ states using the correct order of increasing calculated excitation energies. An improved agreement would be obtained, when the 2_2^+ and 2_4^+ states are identified in reversed order with the known states, as given in Table II. In this case at least the 2_4^+ state would receive a large amplitude as observed experimentally, but then the calculated excitation energies deviate strongly from the experimental values.

The band head of the $K^\pi = 2_2^+$ band [16] has obviously only a very small overlap with the ground state of ^{12}C. On the other hand, in the ^{10}B(^{3}He,t)^{10}Be reaction [22] the Gamow-Teller (GT) transitions from the ^{10}B(3^+) ground state populate the 2_2^+ state as the *strongest* line from in total three observed states. The two others are (i) the 2_1^+ state at 3.37 MeV, which has the lowest cross section, and (ii) a state at 9.4 MeV tentatively assigned as the 3^+ member of the $K = 2$ band. Millener [16] showed explicitly the strong parentage of the 2_2^+ state to the ^{10}B ground state. This clearly indicates a different structure between the 2_2^+ state and the 0_1^+ and 2_1^+ states of ^{10}Be. Pieper, Varga, and Wiringa performed QMC calculations [14] and extracted the deformations of the 2_1^+ and 2_2^+ states at 3.37 MeV and 5.96 MeV, respectively: the first one has a negative quadrupole deformation, but the 2_2^+ state a positive one. They also obtain the first 3^+ state at about the experimental binding energy. This 3_1^+ state has the same strong prolate deformation as the 2_2^+ state.

In the ^{12}C(^{12}C,^{14}O)^{10}Be reaction the small cross section for the 2_2^+ state can be explained in addition by a partial cancellation between two different transition branches. Besides the direct one-step transfer (Fig. 4 and Table I, row 3a) a second branch, which populates this state in a two-step process via the inelastic excitation of the 2_1^+ state of ^{12}C, has been included. Here the proton pair is transferred in the second step with $\ell = 0$ and $\ell = 2$. It turns out that this second branch cancels in part the contributions from the first branch by destructive interference.

2. The odd-parity states at 5.96 MeV and 7.37 MeV

Two transfer branches are taken into account for the transitions to the 1^- and 3^- odd-parity states:

(i) the two-step transitions with ℓ-transfers as specified in Table I, rows 4a, 5a, 9a, via the 3_1^- state of ^{12}C (Fig. 4) and
(ii) the direct transfer of a proton-pair with odd angular momentum transfer ℓ (rows 4b, 5b, 9b), as discussed in Sec. III B. The corresponding branches are shown in the coupling scheme as dashed (red) lines with the angular momentum transfers $\ell = 1$ or 3.

For the latter transfer branches the spectroscopic product A_ℓ has not been used as free variable in the fit, but with the constant value $|A_\ell| = 0.30$. This has been derived from the upper limit of the experimental (2p-2h) strength in the ^{12}C ground state given in Sec. III B and the spectroscopic factor SMAG(proj)= 0.60 [37] of the projectile transition. Therefore it represents an upper limit of A_ℓ for this transfer branch. The sign of A_ℓ has a visible effect on the oscillatory structure of the calculated angular distribution due to the interference of this amplitude with the reaction amplitude from the two-step branch (i). With a minus sign the phase of the observed angular structure is reproduced the best in all cases (Fig. 3 and Table I, rows 4b, 5b, 9b).

The contributions from the two different transfer branches for the 1_1^- state at 5.96 MeV are shown explicitly in Fig. 6.

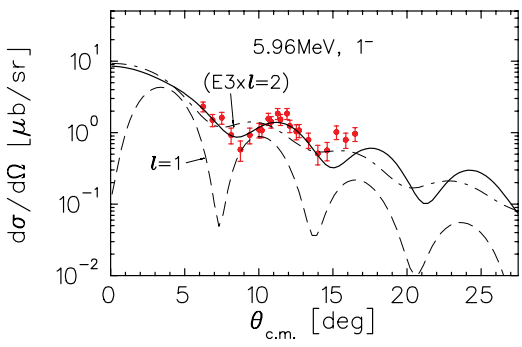

FIG. 6. (Color online) Contributions of the different transfer branches to the angular distribution of the 1^- state at 5.96 MeV. The dot-dashed line shows the contribution from the branch via the ^{12}C(3^-) excitation followed by the two-proton pickup with $\ell = 2$ indicated as ($E3 \times \ell = 2$). The direct $\ell = 1$ transition is shown as long-dashed line. The solid line represents the *coherent* sum of both reaction amplitudes.

The angular distribution of the two-step transition [branch (i)] indicated by ($E3 \times \ell = 2$) in Fig. 6 almost reproduces the height of the experimental cross sections, but the phase of the oscillatory structure is not correct (dot-dashed line). For the angular distribution of the direct pair transfer, which is indicated by $\ell = 1$ in Fig. 6, the oscillatory structure is by far too deep, and the phase is also in this case not correct. However, the data are well described by the coherent sum of the reaction amplitudes (solid line).

For the experimental angular distribution at 7.37 MeV [Fig. 3(d)] it is clear, although there are large statistical fluctuations, that the shape for the 2^+_3 state at 7.54 MeV does not fit the data at all due to its deep oscillatory structure [Fig. 3(d), short-dashed line], whereas the angular distribution of the 3^-_1 state fits reasonably well (solid line). For the transition to the 2^+_3 state at 7.54 MeV an upper limit of $A_{\ell=2} < 0.3$ is estimated for the spectroscopic product.

The only adjustable variable in the fit of the experimental 1^- and 3^- angular distributions by the coupled-channels calculations is the spectroscopic product of the two-proton transfer in the second step of the two-step branch (i) (Fig. 4), following the $E3$ excitation in ^{12}C (see the underlined values in Table I, rows 4a, 5a, 9a). A spectroscopic product $A_{\ell=2} = 1.00$ is obtained for the transition to the 1^- state. The value is very similar to most of the other two-proton spectroscopic products, whereas for the 3^- state at 7.37 MeV it is somewhat smaller (0.63).

In the coupled-channels calculations for the 1^-_1 state an $E1$ transition with the $0^+_{\text{g.s.}} \rightarrow 1^-_1$ excitation in ^{10}Be, after the two-proton pickup to its ground state, might be included. Experimental information about the $E1$ strength for the $1^-_1 \rightarrow 0^+_{\text{g.s.}}$ γ-transition has been derived from data of the ^{11}Li β-decay [38,39]. A lifetime of 330(130) fs [38] has been deduced from the line shape analysis of the corresponding broadened peak in the γ-ray spectrum, after the β-decay of ^{11}Li and the neutron-emission from the ^{11}Be states to excited states of ^{10}Be. The line shape depends on the lifetime through the Doppler broadening according to the competition between the slowing-down time of the excited ^{10}Be in the stopping material and the γ-emission within the lifetime of the state. But there exist considerable systematic errors for the actual case to extract the lifetime for the 1^-_1 state due to the nearby unresolved γ-ray from the 2^+_2 state to the ground state, uncertainties about the possible $1^-_1 \rightarrow 2^+_2$ decay [however, the $1^-_1 \rightarrow 0^+_1/2^+_1$ branching has been measured: 74(5)%/26(10)%], the small relative intensities of the γ-transitions to the ground and 2^+_1 states, and the not very well known feeding pattern from the ^{11}Be neutron-decay, which have a strong influence on the time dependence of the Doppler broadening.

Fynbo *et al.* [38] deduced for the γ-decay to the ground state a $B(E1)\downarrow$ value of $7(3) \times 10^{-6}\, e^2\text{fm}^2$ taking the extracted lifetime and the branching ratio of the decay to the 0^+_1 state and 2^+_1 state of ^{10}Be into account. In view of the large systematic errors we may use an estimate in the range of $(2\text{–}8) \times 10^{-5}$ for the $B(E1)\uparrow$ value to excite the 1^-_1 state. A corresponding transfer branch with an inelastic excitation in the second step of this $B(E1)\uparrow$ strength gives only negligible contributions to the final cross sections and has not been taken into account. We found in test calculations, that the cross sections of the 1^- state might be reproduced with $B(E1)\uparrow$ values of 0.03–0.05 $e^2\text{fm}^2$, which are about three orders of magnitude larger than the values from Fynbo *et al.* [38].

Theoretical calculations for $B(E1)\uparrow$ values of this $E1$ transition are only slightly larger as compared to the $B(E1)\uparrow$ estimate obtained from our test calculations: Kanada-En'yo and Kimura obtain $B(E1)\uparrow = 0.06\, e^2\text{fm}^2$ [40], and Itagaki and Okabe $B(E1)\uparrow = 0.072\, e^2\text{fm}^2$ [5].

Sarazin *et al.* [39], who performed similar measurements and analyses of the ^{11}Li β-decay, did not publish a definite value for the lifetime of the 1^-_1 state in view of the above-mentioned difficulties. The authors gave only an upper limit of a few hundred femto-seconds for the lifetime of this state, which is consistent with the value of Ref. [38].

3. *States of the peak at 9.5 MeV*

The experimental angular distribution of the peak at 9.5 MeV [Fig. 3(e)] has been fitted using contributions from three states known in this region [11,20–23,30,31]. The phase of the observed oscillatory pattern is determined by the 2^+_4 state at 9.56 MeV as the dominant contribution [dashed line in Fig. 3(e)], but the minima in the corresponding calculated angular distribution are too deep. These can be filled by additional contributions from other states, which are out of phase with this angular structure. Two states are relevant in this case: the first one is a 4^- state at 9.27 MeV [11,30,31], which shows this behavior (dot-dashed line). The second one could be the 3^+ state predicted in SM calculations in this excitation energy region [13,15,16], which is, however, up to now only tentatively identified with a state reported in the ^{10}B(t,^{3}He) reaction at 9.4 MeV [22] (Table I). This state is also observed in the ^{10}B(d,^{2}He) reaction at the slighly lower excitation energy of 9.3 MeV [23]. In the compilation of Tilley *et al.* [20] it is assumed that the state at 9.40 MeV might be identified with the 2^+_4 state at 9.56 MeV, but the 160 keV difference in excitation energy is rather large and indicates most probably a different state. SM calculations [15,16] consistently support a tentative assignment of (3^+) for the observed strength and also recent cluster-model calculations (see, e.g., [4,6–8]).

We performed fits to the data at 9.5 MeV in three different ways using in all cases the angular distribution of the 2^+_4 state as the dominant part and, in addition, the distributions either (i) from the 4^- state, or (ii) from the tentative 3^+ state or (iii) from both of these states. In least-χ^2 fits the following χ^2-values per degrees-of-freedom were obtained: (i) $\chi^2(2^+, 4^-) = 1.38$; (ii) $\chi^2(2^+, 3^+) = 1.14$; (iii) $\chi^2(2^+, 4^-, 3^+) = 1.00$. It turns out that the fit is improved considerably in the cases, when the 3^+ state is included. The result of the best fit is shown in Fig. 3(e), where all three angular distributions are used, the sum is displayed as the solid line.

The corresponding spectroscopic products A_ℓ determined in the fit for the transitions to the $2^+, 4^-$ and 3^+ states are given in Table I in rows 6, 7, and 8, respectively. All three A_ℓ-values are in the range of 1.02 ± 0.10 and very similar to the $A_{\ell=2}$ value for the first excited 2^+ state of ^{10}Be. It seems that the reaction step of the two-proton transfer is described correctly (and quantitatively) in all these cases with a single $\ell = 2$ transfer amplitude of approximately the same strength.

4. Assignments for the states at 10.55 MeV and 11.8 MeV

In the comparison of the experimental angular distributions at 10.55 MeV [Fig. 3(f)] and at 9.5 MeV [Fig. 3(e)] a clear out-of-phase behavior is seen. Since the spin and parity of the 2^+ state at 9.56 MeV is well established [20] and also confirmed by our analysis, an angular distribution with the shape for a $J^\pi = 3^-$ state has been compared to the data at 10.55 MeV and an excellent agreement is found. This is not only true for the general shape of the oscillatory structure, but also for the characteristic position of the first deep diffraction minimum. This agreement allows a definite assignment of $J^\pi = 3^-$ for this state. It is populated with two branches, in the same way as the 3^- state at 7.37 MeV: (i) with a two-step branch via the $E3$ excitation of the ^{12}C(3^-) state at 9.64 MeV followed by the transfer of the proton pair with $\ell = 0, 2$ and with a spectroscopic product of $A_\ell = 0.80$ (Table I, row 9a), and (ii) by the direct two-proton transfer with angular momentum transfer $\ell = 3$ (row 9b). Some details for this state were also already given in Sec. III D2 in the discussion of the odd-parity states.

It is intriguing to compare the angular distribution of the state at 10.55 MeV also with the shape for an angular distribution of a 3^+ state [Fig. 3(f), dotted line], which is available already from the 9.4 MeV state. We notice, that this shape is in phase with the observed structure at 10.55 MeV, at least within the measured range of the data. Significant differences can be seen only at more forward angles. But the fit with this shape is not as good as for the 3^- distribution, although a possible (3^+) assignment might not be completely excluded. A 3^+ state would be populated in two steps via the first excited 2^+ state of ^{12}C and the two-proton pickup with an $\ell = 2$ transfer (Table I, row 10).

The angular distribution of the peak at 11.8 MeV shows an extended flat shape at forward angles and drops only at $\theta_{\text{c.m.}} \sim 12^\circ$ with a shallow minimum at about 15°. From the comparison to the other already calculated angular distributions we conclude, that the spin must be larger than $J = 3$. The first (deep) minimum of a calculated 3^- distribution is located at a smaller scattering angle, at about 13.0°. The comparison of the data to the calculated angular distributions for $J^\pi = 4^+$ and 5^- [Fig. 3(g)] shows, that only the shape for the 4^+ state is consistent with the data, the angular structure for a 5^- assignment does not fit. The angular distribution for $J^\pi = 4^+$ is calculated with an inelastic excitation of the ^{12}C(2_1^+) state and a two-proton pickup in the second step with $\ell = 2$ (Table I, row 11). The excitation energy of this state fits well to the expected position for the 4^+ member of the ground-state band, when the dependence of the excitation energy on $J(J+1)$ is extrapolated from the 2^+ state at 3.37 MeV to $J^\pi = 4^+$. At 11.8 MeV it is the second 4^+ state of ^{10}Be, because a lower-lying 4^+ state exists at $E_x = 10.15$ MeV (a member of the molecular band [10]).

Calculations within different models for ^{10}Be localize the 4^+ member of the ground-state band at the following excitation energies: antisymmetrized molecular dynamics (AMD) at 9.93 MeV [4], molecular orbital model (MOM) 12.9 MeV* [5], semi-microscopic algebraic cluster model (SACM) 10.74 MeV [6], multicluster generator coordinate method (MCGCM) 11.1 MeV [7], microscopic four-cluster model of ^{10}Be (MFCM) 11.74 MeV* [8], generalized two-center cluster model (GTCM) 12.0 MeV [9] (for the excitation energies *marked by MeV** the $\alpha + \alpha + n + n$ threshold at 8.386 MeV was taken as the reference energy, not the calculated ground state energy). This list does not claim to be complete, it rather gives an impression of the agreement between the different models. Most of the cited theoretical predictions come close to the excitation energy of the state, which is now firmly assigned as 4^+ in this measurement.

The structure of the two known 4^+ states, the first at 10.15 MeV (4_1^+ [10]), and the second at 11.8 MeV (4_2^+, this work), must be very different, since the 4_2^+ state is well observed in the ^{12}C(^{12}C,^{14}O)^{10}Be reaction, whereas this is not the case for the 4_1^+ state.

The 4_1^+ state has been identified recently [10] as a member of the molecular rotational band based on the 0_2^+ state at 6.18 MeV, which has a very pronounced $\alpha : 2n : \alpha$ cluster structure with large extension and strong decay width to the ^{6}He+α channel. This state is strongly populated in reactions like ^{7}Li(^{7}Li;α,^{6}He)α [12], whereas this is not the case for the 4_2^+ state. The opposite behavior is observed in reactions, which do not have a special selectivity for the formation of cluster structures, for example the ^{12}C(^{12}C,^{14}O) reaction used in this work, or the ^{7}Li(α, p)^{10}Be reaction [11].

The latter reaction is populating almost all known states up to 12 MeV excitation energy [20] (with the only exceptions of the 2^- and (3^+) states at 6.26 MeV and 9.4 MeV, respectively) without a clear selectivity for different structures. But it is interesting, that the two strongest states in the (α, p) spectrum are the 2_1^+ state at 3.37(5) MeV and the state at 11.76(7) MeV, which Hamada *et al.* [11] already tentatively assigned (4^+) and which corresponds to the 11.8(1) MeV state in the present work. The large cross sections for these states in the (α, p) reaction, our definite 4^+ assignment for the 11.8 MeV state, the agreement of this excitation energy for the 4^+ state with the $J(J+1)$ systematics for rotational bands and the weak population in reactions with a high selectivity for a ^{6}He $\otimes$ α cluster structure supports the identification of the 11.8 MeV state as a member of the ground state rotational band of ^{10}Be.

E. Band structures in ^{10}Be

The relation $E_x(J) = E_{x,0} + a(K^\pi) \times J(J+1)$ between excitation energies E_x and spins J, with the K^π quantum number of the band head and the slope parameter $a(K^\pi) = \hbar^2/2\theta$, has been used to deduce more detailed information for the different bands. The slope parameter contains the moment-of-inertia θ of the rotating mass distribution. A value $a(0_1^+) = 560$ keV is deduced for the $K^\pi = 0_1^+$ ground-state band (members: 0_1^+, 0.00 MeV; 2_1^+, 3.37 MeV; 4_2^+, 11.78 MeV). The band is shown in Fig. 7.

As compared to the molecular rotational band (members: 0_2^+, 6.18 MeV; 2_3^+, 7.54 MeV; 4_1^+, 10.15 MeV, Fig. 7), which has a very shallow slope with $a(0_2^+) = 200$ keV and a large moment-of-inertia, the mass distribution for the members of the ground-state band, which is deduced from the much bigger slope parameter $a(0_1^+) = 560$ keV, must be more compact. Using the simple picture for the mass distributions

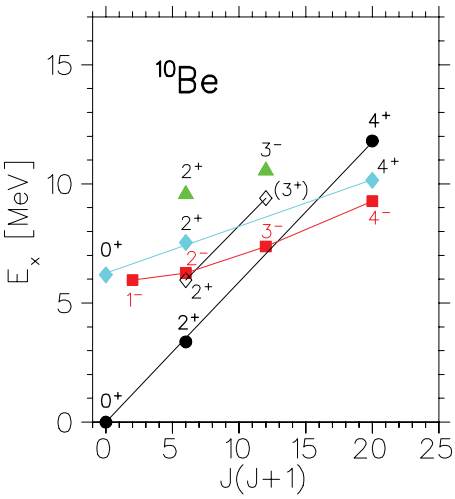

FIG. 7. (Color online) Band structure of ^{10}Be states up to angular momenta of $J = 4$. Four bands are shown: the ground-state band (black circles), a $K = 2^+_2$ band (open diamonds), the $K = 1^-_1$ band (red sqares), and the $K = 0^+_2$ molecular band (blue filled diamonds). Other known states at 9.56 MeV (2^+_4) and 10.55 MeV (3^-_2) are plotted as single points (two filled triangles).

of two neutrons and two α-particles represented by Gaussian density distributions at a variable distance D_α to reproduce the slope parameter, very different values for the distance D_α are obtained, 2.7 fm for the $K^\pi = 0^+_1$ band and 5.9 fm for the 0^+_2 band. Yet the deformation parameter for the ^{10}Be ground-state band obtained from inelastic scattering is $\beta_2 = 1.13$ [17], it is one of the largest values observed.

A $K^\pi = 2^+_2$ band is predicted by many theoretical models [4–6,8,13,14,16], with only two members: 2^+_2 and 3^+_1. The band head is localized in the region between excitation energies of 4.5 MeV and 7.0 MeV. The experimental members of this band can be identified with the known 2^+_2 state at 5.96 MeV as the band head and the (3^+) state at 9.40 MeV ([22] and this work). The value $a(K^\pi = 2^+_2) = 570$ keV for the slope parameter is almost the same as for the ground-state band. The $K^\pi = 2^+_2$ band is displaced in parallel by about 2.59 MeV to higher excitation energies with respect to the ground-state band. But its structure is different, as one can see, e.g., from the QMC calculations [14] (see Sec. III D1). The ground-state band is strongly populated in the two-proton pick-up reaction ^{12}C(^{12}C,^{14}O), whereas this is not the case for the $K^\pi = 2^+_2$ band.

From the $K^\pi = 1^-_1$ odd-parity band with the members (discussed here up to $J = 4$): 1^-_1, 5.96 MeV; 2^-, 6.26 MeV; 3^-, 7.37 MeV; 4^- 9.27 MeV, only the states with natural parity, 1^- and 3^-, are well populated in the ^{12}C(^{12}C,^{14}O) reaction, whereas the 2^- state could not be identified in the spectrum and the 4^- state only indirectly by unfolding the angular distribution of the peak at 9.5 MeV. As mentioned already in Sec. III B, the structure of this band is described by a main configuration of $^9\text{Be}_{\text{g.s.}} \otimes \nu(2s1d)^1$ [30,31]. The excitation energies in this band do not very well follow a linear dependence on $J(J+1)$. A mean value for the slope parameter of $a(1^-_1) = 250$ keV is obtained.

The three band heads of the $K^\pi = 0^+_2$, 1^-_1, and 2^+_2 bands are weakly bound states with binding energies with respect to the neutron threshold ($S_n = 6.812$ MeV) of only 0.633 MeV, 0.852 MeV and 0.854 MeV, respectively. The structure of these band heads is well illustrated for example by the calculations within the microscopic four-cluster model of Koji Arai (Fig. 3 in Ref. [8]), where the correlation discussed above between the slope parameters $a(K^\pi)$ and the extention of the form factors is visible.

IV. CONCLUSIONS

The two-proton pick-up reaction ^{12}C(^{12}C,^{14}O) has been used at an incident energy of 211.4 MeV to study the structure of states of ^{10}Be up to 12 MeV excitation energy. Spin-parity assignments have been obtained from the characteristic shapes of the observed angular distributions and two new assignments could be made. The states at 10.55 MeV and 11.8 MeV excitation energy have been firmly assigned as 3^- and 4^+, respectively, and the latter has been identified as the 4^+ member of the ground-state band. The coupled-channels calculations describe the pronounced structures and the cross sections of the experimental angular distributions consistently with spectroscopic products for the two-proton pickup of about the same strength for most of the cases.

The natural-parity members of the 1^-_1 band at 5.96 MeV have been populated with good cross sections, which are also quantitatively described using two reaction steps for the main transition branch, first the inelastic excitation to the 3^-_1 state of ^{12}C, and second, the pickup of the proton pair. Experimental cross sections for the 2^+_2 state at 5.96 MeV are an order of magnitude smaller than for the 1^-_1 state. The 2^+_2 state forms together with the tentatively assigned (3^+) state at 9.4 MeV a $K^\pi = 2^+$ band.

ACKNOWLEDGMENTS

The authors thank the ISL accelerator staff for the stable operation of the accelerators. C.W. is grateful for the support of the Alexander von Humboldt Stiftung.

[1] K. Ikeda, N. Tagikawa, and H. Horiuchi, Prog. Theor. Phys. Suppl. Extra Number, 464, (1968).
[2] H. Horiuchi, K. Ikeda, and Y. Suzuki, Prog. Theor. Phys. Suppl. **52**, 89 (1972).
[3] W. von Oertzen, Z. Phys. A **357**, 355 (1997).
[4] Y. K. Kanada-En'yo, H. Horiuchi, and A. Doté, Phys. Rev. C **60**, 064304 (1999).
[5] N. Itagaki and S. Okabe, Phys. Rev. C **61**, 044306 (2000).
[6] L. Hernández de la Peña, P. O. Hess, G. Lévai, and A. Algora, J. Phys. G **27**, 2019 (2001).
[7] P. Descouvemont, Nucl. Phys. **A699**, 463 (2002).
[8] Koji Arai, Phys. Rev. C **69**, 014309 (2004).
[9] M. Ito, K. Kato, and K. Ikeda, Phys. Lett. **B588**, 43 (2004).
[10] M. Freer, E. Casarejos, L. Achouri, C. Angulo, N. I. Ashwood, N. Curtis, P. Demaret, C. Harlin, B. Laurent, M. Milin, N. A. Orr, D. Price, R. Raabe, N. Soić, and V. A. Ziman, Phys.

Rev. Lett. **96**, 042501 (2006); See also M. Milin, M. Zadro, S. Cherubini, T. Davinson, A. Di Pietro, P. Figuera, D. Miljanić, A. Musumarra, A. Ninane, A. N. Ostrowski, M. G. Pellegriti, A. C. Shotter, N. Soić, and C. Spitaleri, Nucl. Phys. **A753**, 263 (2005).

[11] S. Hamada, M. Yasue, S. Kubono, M. H. Tanaka, and R. J. Peterson, Phys. Rev. C **49**, 3192 (1994).

[12] N. Curtis, N. I. Ashwood, N. M. Clarke, M. Freer, C. J. Metelko, N. Soić, W. N. Catford, D. Mahboub, S. Pain, and D. C. Weisser, Phys. Rev. C **70**, 014305 (2004); N. Curtis, N. I. Ashwood, L. T. Baby, T. D. Baldwin, T. R. Bloxham, W. N. Catford, D. D. Caussyn, M. Freer, C. W. Harlin, P. McEwan, D. L. Price, D. Spingler, and I. Wiedenhover, *ibid*. **73**, 057301 (2006).

[13] E. Caurier, P. Navrátil, W. E. Ormand, and J. P. Vary, Phys. Rev. C **66**, 024314 (2002).

[14] Steven C. Pieper, K. Varga, and R. B. Wiringa, Phys. Rev. C **66**, 044310 (2002).

[15] S. Cohen and D. Kurath, Nucl. Phys. **A101**, 1 (1967).

[16] D. J. Millener, Nucl. Phys. **A693**, 394 (2001).

[17] S. Raman, C. H. Malarkey, W. T. Milner, C. W. Nestor, Jr., and P. H. Stelson, At. Data Nucl. Data Tables **36**, 1 (1987).

[18] H. G. Bohlen, R. Kalpakchieva, A. Blažević, B. Gebauer, T. N. Massey, W. von Oertzen, and S. Thummerer, Phys. Rev. C **64**, 024312 (2001).

[19] A. G. Drentje, H. A. Enge, and S. B. Kowalski, Nucl. Instrum. Methods **122**, 485 (1974).

[20] D. R. Tilley, J. H. Kelly, J. L. Godwin, D. J. Millener, J. E. Purcell, C. G. Sheu, and H. R. Weller, Nucl. Phys. **A745**, 155 (2004).

[21] U. Schwinn, G. Mairle, G. J. Wagner, and Ch. Rämer, Z. Phys. A **275**, 241 (1975).

[22] I. Daito, H. Akimune, S. M. Austin, D. Bazin, G. P. A. Berg, J. A. Brown, B. S. Davids, Y. Fujita, H. Fujimura, M. Fujiwara, R. Hazama, T. Inomata, K. Ishibashi, J. Jänecke, S. Nakayama, K. Pham, D. A. Roberts, B. M. Sherrill, M. Steiner, A. Tamii, M. Tanaka, H. Toyokawa, and M. Yosoi, Phys. Lett. **B418**, 7 (1998).

[23] T. Inomata, H. Akimune, I. Daito, H. Ejiri, H. Fujimura, Y. Fujita, M. Fujiwara, M. N. Harakeh, K. Ishibashi, H. Kohri, N. Matsuoka, S. Nakayama, A. Tamii, M. Tanaka, H. Toyokawa, M. Yoshimura, and M. Yosoi, Phys. Rev. C **57**, 3153 (1998).

[24] M. L. Roush, F. C. Young, P. D. Forsyth, and W. F. Hornyak, Nucl. Phys. **A128**, 401 (1969).

[25] I. P. Thompson, Comput. Phys. Rep. **7**, 167 (1988).

[26] P. J. Simmonds, K. I. Pearce, P. R. Hayes, N. M. Clarke, R. J. Griffiths, M. C. Mannion, and C. A. Ogilvie, Nucl. Phys. **A428**, 653 (1988).

[27] P. B. Foot, D. Barker, C. O. Blyth, J. B. A. England, O. Karban, M. C. Mannion, J. M. Nelson, C. A. Ogilvie, C. Pinder, L. Potvin, S. Roman, G. G. Shute, L. Zybert, R. Zybert, J. M. O'Donnell, M. J. Smithson, N. M. Clarke, K. I. Pearce, P. Simmonds, and B. M. Spicer, J. Phys. G **13**, 1531 (1987).

[28] H. T. Fortune, D. J. Crozier, B. Zeidman, and M. E. Cobern, Nucl. Phys. **A303**, 14 (1978).

[29] G. van der Steenhoven, H. P. Blok, J. W. A. den Herder, E. Jans, P. H. M. Keizer, L. Lapikas, E. N. M. Quint, P. K. A. de Witt Huberts, G. W. R. Dean, P. J. Brussaard, P. W. M. Glaudemans, and D. Zwarts, Phys. Lett. **B156**, 151 (1985).

[30] R. E. Anderson, J. J. Kraushaar, M. E. Rickey, and W. R. Zimmermann, Nucl. Phys. **A236**, 77 (1974).

[31] H. G. Bohlen, W. von Oertzen, A. Blažević, B. Gebauer, M. Milin, Tz. Kokalova, Ch. Schulz, S. Thummerer, A. Tumino, R. Kalpakchieva, T. N. Massey, and S. M. Grimes, in *Proceedings of the International Symposium on Exotic Nuclei*, Baikal Lake (Russia), July 2001, edited by Yu. E. Penionzhkevich and E. A. Cherepanov (World Scientific, Singapore, 2002), p. 453.

[32] C. B. Fulmer, G. R. Satchler, K. A. Erb, D. C. Hensley, R. L. Auble, J. R. Ball, F. E. Bertrand, and E. E. Gross, Nucl. Phys. **A427**, 545 (1984).

[33] K. W. Jones, C. Glashausser, R. deSwiniarski, S. Nanda, T. A. Carey, W. Cornelius, J. M. Moss, J. B. McClelland, J. R. Comfort, J.-L. Escudie, M. Gazzaly, N. Hintz, G. Igo, M. Haji-Saeid, and C. A. Whitten, Jr., Phys. Rev. C **33**, 17 (1986).

[34] P. M. Endt, At. Data Nucl. Data Tables **23**, 3 (1979).

[35] D. L. Auton, Nucl. Phys. **A157**, 305 (1970).

[36] H. Iwasaki, T. Motobayashi, H. Akiyoshi, Y. Ando, N. Fukuda, H. Fujiwara, Zs. Fülöp, K. I. Hahn, Y. Higurashi, M. Hirai, I. Hisanaga, N. Iwasa, T. Kijima, A. Mengoni, T. Minemura, T. Nakamura, M. Notani, S. Ozawa, H. Sakurai, S. Shimoura, S. Takeuchi, T. Teranishi, Y. Yanagisawa, and M. Ishihara, Eur. Phys. J. A **13**, 55 (2002).

[37] S. Cohen and D. Kurath, Nucl. Phys. **A141**, 145 (1970).

[38] H. O. U. Fynbo, M. J. G. Borge, J. Cederkäll, S. Courtin, P. Dessagne, B. Jonson, G. Le Scornet, T. Nilsson, G. Nyman, E. Poirier, K. Riisager, O. Tengblad, K. Wilhelmsen, and ISOLDE Collaboration, Nucl. Phys. **A736**, 39 (2004).

[39] F. Sarazin, J. S. Al-Khalili, G. C. Ball, G. Hackman, P. M. Walker, R. A. E. Austin, B. Eshpeter, P. Finlay, P. E. Garrett, G. F. Grinyer, K. A. Koopmans, W. D. Kulp, J. R. Leslie, D. Melconian, C. J. Osborne, M. A. Schumaker, H. C. Scraggs, J. Schwarzenberg, M. B. Smith, C. E. Svensson, J. C. Waddington, and J. L. Wood, Phys. Rev. C **70**, 031302(R) (2004).

[40] Y. Kanada-En'yo and M. Kimura, Phys. Rev. C **72**, 064301 (2005).